Evolution of excess pore water pressure in undrained clay-structure interface shear tests

Alejandro Martinez[1#] and *Hans Henning* Stutz[2]

[1]*University of California Davis, Department of Civil and Environmental Engineering, 2001 Ghausi Hall, Davis CA, USA*
[2] *Institute of Soil mechanics and Rock mechanics, Karlsruhe institute of technology, Engler-Bunte-Ring 14 76131 Karlsruhe, Germany*
[#]*Corresponding author: amart@ucdavis.edu*

ABSTRACT

Recent studies focused on the shear behaviour of clay-structure interfaces have shown the importance of the shearing rate on the strength of these interfaces. In normally-consolidated clays, increasing the shearing rate results in a decrease in the interface strength, while the trend is opposite in heavily overconsolidated clays. While analytical and empirical interpretation methods indicate that the generation of shear-induced excess pore pressures are responsible for the aforementioned trends, experiments with pore water pressure measurements at the clay-structure interface are rare. In this paper, we first describe a modified interface shear box testing setup that is equipped with a pore water pressure sensor. For this equipment, the fully rough structural surface was manufactured with a port at the centre of the clay-surface interface to measure the pore water pressure. We present the results of undrained clay-structure interface tests on normally consolidated (NC) and overconsolidated (OC) specimens of kaolin clay. The results agree with the expectations, where the NC specimens generate excess pore pressures with greater magnitudes and heavily OC specimens generate negative excess pore pressures. Measurements of the pore water pressures allow calculating vertical effective stresses, which can be used to investigate the effective stress paths followed by the clay-structure interface during the tests. This paper also provides a comparison of the measured values of beta and adhesion factors with previously published results and relationships used for the design of deep foundations.

Keywords: Soil-structure interface behaviour; fine-grained soils; excess pore water pressure.

1. Introduction and background

The interface shear strength between soils and structures is a parameter required for the engineering design of structures like deep foundations and soil nail systems. Previous research has shown the dependency of the mobilized interface strength on the rate of deformation (e.g. Jardine and Lehane 1992; Lemos and Vaughan 2000). This dependency is due to the generation of excess pore pressures, with fast deformation rates leading to undrained conditions, slow rates to drained conditions, and intermediate rates to partially-drained conditions (e.g. Boukpeti and White 2017; Martinez and Stutz 2019). To exemplify this behaviour, Fig. 1a-1c shows the results of interface shear tests between Kaolin clay specimens and a rough surface. The mobilized shear stress (τ) decreases as the shearing velocity (v) is increased for normally consolidated (NC) specimens due to the generation of positive excess pore pressures (Δu). For the overconsolidated (OC) specimens, τ increases as v is increased due to the generation of negative Δu. While this behaviour has been observed experimentally and modelled analytically, there is uncertainty of the magnitudes of Δu developed, resulting in challenges in determining the drainage conditions. Additionally, when the conditions are not fully drained, the interpretation is typically limited to the total stress framework.

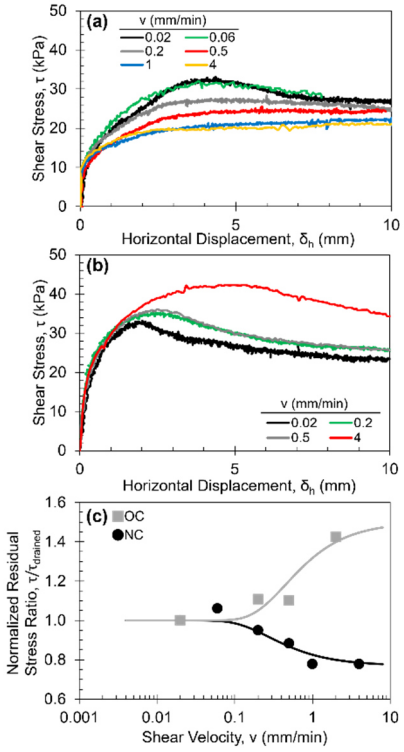

Figure 1. Shear stress at different shearing velocities for (a) NC and (b) OC (OCR = 5) soils. (c) Relationships between normalized residual stress ratio and shearing velocity (data from Martinez and Stutz 2019).

This paper describes a novel interface shear setup equipped with a port to measure the pore pressure generated at the clay-structure interface. Results of tests on samples with varying overconsolidation ratios (OCR) are presented. Finally, parameters for the design of deep foundations are deduced to exemplify the usefulness of measuring the pore pressures during interface shear tests.

2. Materials and methods

2.1. Interface shear tests with pore pressure measurements

A custom-built interface shear setup was built to allow for pore pressure measurements at the clay-surface interface. The new setup is shown in Fig. 2. The shear box, testing surface and bottom plate were constructed out of aluminium. A porous element with a diameter of 10 mm is mounted on the testing surface. Below the porous element there is a small channel that leads to a port in the base plate to which the pore pressure transducer is connected. An O-ring between the testing surface and the bottom plate provides proper sealing to avoid water leakage. The testing surface and bottom plate are attached with four setscrews that compress the aforementioned O-ring. The vertical load is applied with a piston on the loading cap while the horizontal load is applied with a loading arm. Both vertical and horizontal forces are measured with load cells, while an LVDT is used to measure the vertical displacement of the load cap. The specimen diameter is 80 mm and its height is between 30 and 40 mm.

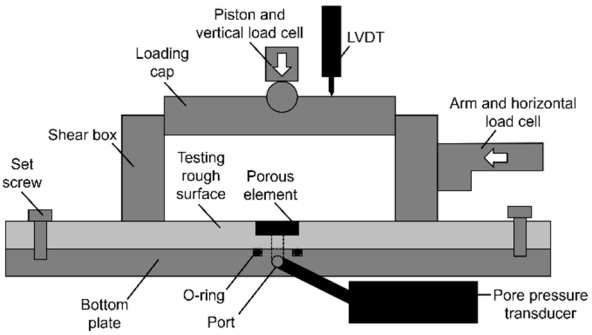

Figure 2. Schematic of interface shear setup with pore pressure measurements.

The testing surface and porous element were sand blasted with the same blasting media with the goal of matching the magnitude of their surface roughnesses. However, due to the large pores in the porous element, the resulting surface roughness was different. Fig. 3a shows a 3D scan of the central portion of the testing surface with the porous element, while Figs. 3b and 3c show X – Z profiles along cross-sections A-A' and B-B'. The 3D scan and X – Z profiles clearly show the differences in the amplitude and wavelength of the asperities. The average surface roughness (R_a) and maximum surface roughness (R_z) for the porous element were measured as 63.3 and 278.4 µm, respectively, while the R_a and R_z values for the testing surface were measured as 10.3 and 77.1 µm, respectively. Fig. 4 compares the relationship between residual shear stress measurements and R_a reported by Martinez and Stutz (2019) with the R_a values of the porous element and surface. The authors performed tests on NC specimens of the same Kaolin clay at slow and fast shearing velocities (i.e. drained and undrained conditions). As shown, the R_a of the porous element and testing surface are within the "fully rough" regime where the interface shear strength is independent of surface roughness. This suggests that the difference in surface roughness has no to little effect because the interface strength is likely the same against the porous element and testing surface.

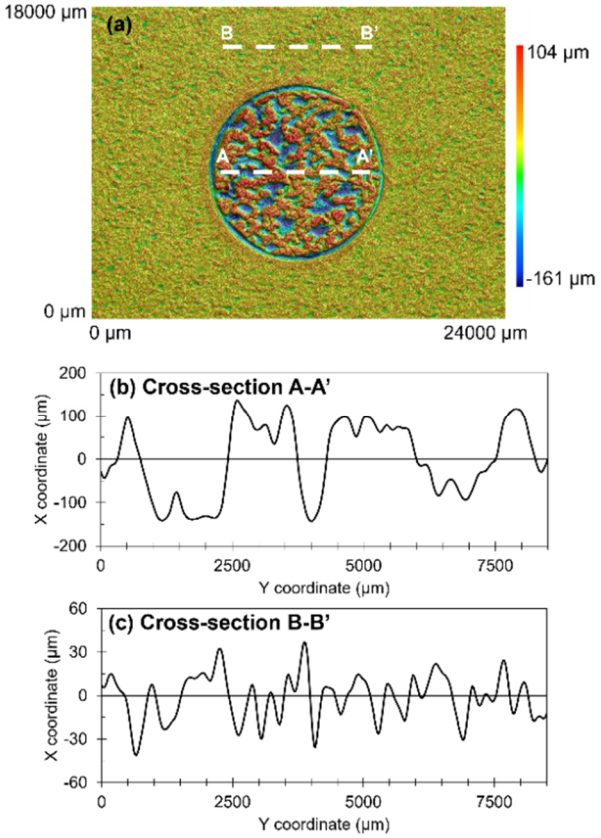

Figure 3. (a) 3D scan of the central portion of the rough testing surface with the porous element and X – Z profiles along cross-sections (b) A-A' along the porous element and (c) B-B' along the testing surface. Note the different y-axis range in (c) and (c).

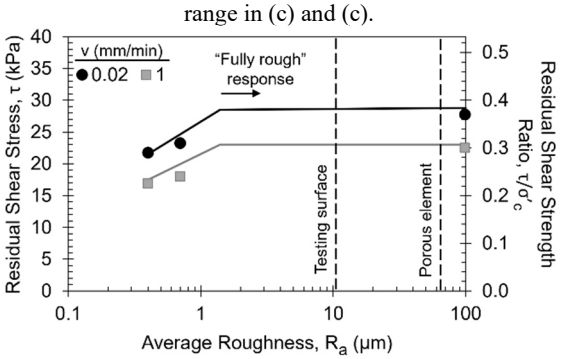

Figure 4. Comparison of the R_a of the porous element and testing surface with the relationship between interface shear strength and R_a (data from Martinez and Stutz 2019).

2.2. Kaolin clay

All the specimens were prepared by pouring a Kaolin slurry with an initial water content equal to 1.5 times the clay liquid limit (L_L) in the shear box. The specimens were then consolidated to the desired effective stress in

the interface shear apparatus. All the specimens were sheared at a rate of 1 mm/min, at which undrained conditions are expected for the NC soil based on Fig. 1 and the analysis by Martinez and Stutz (2019). All the tests were performed at a vertical effective stress at the end of consolidation (σ'_c) of 75 kPa.

The effective failure envelope of the Kaolin clay was determined through direct shear tests is presented in Fig. 5. These tests were performed at a rate at a shearing rate of 0.02 mm/s, which according to the analysis of Martinez and Stutz (2019) ensures drained conditions (Fig. 1). Other relevant properties of the Kaolin are presented in Table 1.

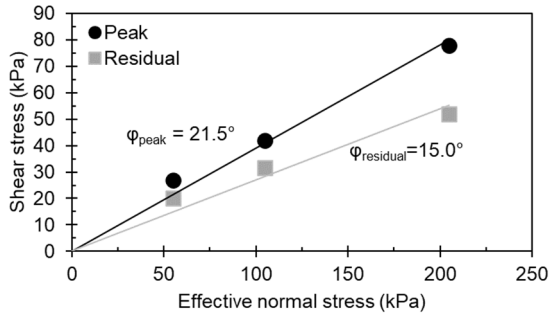

Figure 5. Effective failure envelope of the Kaolin clay determined through direct shear tests.

Table 1. Kaolin clay properties (note: C_V was determined for NC specimens).

Particle specific gravity, G_S	2.66
Liquid limit, L_L (%)	59.8
Plastic limit, P_L (%)	33.9
Compression index, C_c	0.31
Recompression index, C_r	0.14
Coefficient of consolidation, C_V (cm^2/s)	0.007

3. Results

3.1. Shearing response of specimens with varying OCR

Interface shear tests were performed on an NC specimen and on specimens with OCR of 4 and 6 with a v of 1 mm/min and with σ'_c of 75 kPa, as shown in Fig. 6a-6d. As expected, the test on the NC specimen mobilized the smallest shear stresses, while both OC specimens generated similar shear stresses. Specifically, the NC specimen mobilized a maximum shear stress of about 20 kPa accompanied by a strain-hardening response, while the OC specimens mobilized peak shear stresses of about 35 kPa accompanied by a strain-softening response. All specimens experienced positive vertical displacements indicating a reduction in volume, which reflect small amounts of soil exiting the from the back of shear box. Also, small amounts of consolidation could have taken place at the outer perimeter of the specimen where the drainage path is shortest. The OC specimens experienced smaller decreases in volume, likely due larger amount of slippage at the soil-structure interface, as shown by Martinez and Stutz (2019), leading to a smaller amount of soil exiting during shearing.

The excess pore pressures increased with shear displacement for the NC specimen to values as high as 30 kPa, while the specimens with OCR of 4 and 6 mobilized negative Δu of -3 and -6 kPa, respectively. The vertical effective stress (σ'_v) was calculated as the difference between σ'_c and Δu. The σ'_v decreases during shearing for the NC specimen to a value of about 45 kPa due to the positive Δu, while σ'_v increases slightly to values of 78 and 81 kPa for the specimens with OCR of 4 and 6, respectively, due to the negative Δu (Fig. 6d). It is noted that while the tests on the NC specimen is expected to be representative of undrained behaviour, it is possible that the OC specimens could have experienced partially drained conditions due to increase in C_V due to the

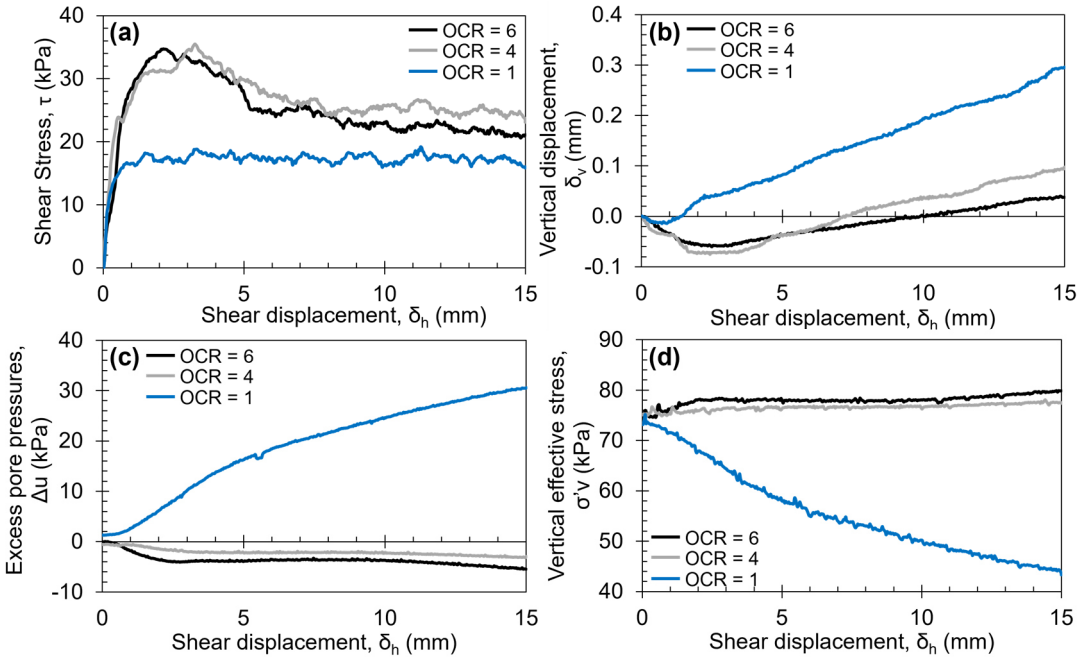

Figure 6. Results of interface shear tests on samples with OCR of 1, 4 and 6: (a) shear stress – shear displacement, (b) vertical displacement – shear displacement, (c) pore pressure – shear displacement and (d) vertical effective stress – shear displacement.

decrease in the clay's compressibility. Nonetheless, these values are assumed to be representative of undrained behavior in the proceeding analysis.

Measurement of Δu allows computing stress ratios (τ/σ'_v) (Fig. 7a). The undrained tests show sharp increases in τ/σ'_v at small shear displacements for the three specimens. The τ/σ'_v of the undrained NC specimen continued to increase with shear displacement, while the OC specimens show a significant decrease after shear displacements between 2.5 and 4 mm. The greater residual τ/σ'_v mobilized by the NC specimen is likely due to the increased amount of slippage at the soil-structure interface that takes place as the OCR is increased, as shown by means of particle image velocimetry (PIV) analysis by Stutz and Martinez (2018). The figure also includes τ/σ'_v values from a drained test on an NC specimen from Martinez and Stutz (2019), showing an initial stiffer response in comparison with the NC undrained test but a similar residual strength.

Computation of σ'_v also allows plotting stress paths for the three tests, as presented in Fig. 7b. The undrained NC specimen shows an initial vertical portion of the stress path caused by the rapid mobilisation of τ at small shear displacements. Once a τ of about 15 kPa is mobilised, the Δu lead to a decrease in σ'_v which results in the stress path sharply turning left. The stress paths for the OC specimens show the mobilised τ peak and subsequent decrease along with the small increases in σ'_v. The figure also shows how the stress paths of the undrained and drained NC specimens converge to the failure envelope for NC Kaolin clay specimens reported by Martinez and Stutz (2019). In contrast, the OC specimens mobilise peak τ that exceed the failure envelope, likely due to their dilative behaviour, while the residual τ values are below the failure envelope due to the slippage at the soil-structure interface.

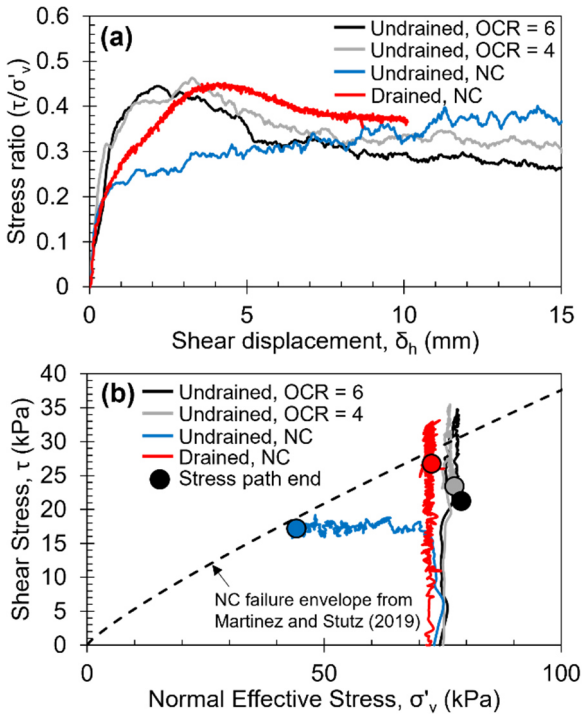

Figure 7. (a) Stress ratio versus shear displacement and (b) effective stress paths for tests on specimens with varying OCR. Drained NC data from Martinez and Stutz (2019).

3.2. Deduction of design parameters from interface shear test results

To exemplify the usefulness of obtaining excess pore pressure measurements, parameters for the design of geotechnical elements within the effective and total stress frameworks are extracted from the test results. For this analysis, the interface shear strength (τ_{int}) is taken as the maximum τ mobilized during each test and the undrained shear strength (S_U) is estimated using the framework by Ladd and Foott (1974), as follows:

$$S_U = S\sigma'_c OCR^m \quad (1)$$

where S and m are constants taken as 0.25 and 0.8, respectively, which are typical values for clays (Ladd and Foott, 1974). The interface shear strength and S_U values are shown in Fig. 8.

The ratio of τ_{int} to σ'_v is equivalent to the β factor used to design deep foundations within the effective stress framework, i.e. $\tau_{int}/\sigma'_v = \beta$. The experimental results are shown in Fig. 9a as a function of OCR, showing the greater τ_{int}/σ'_v for the OC specimens. The figure also shows published values from Esrig and Kirby (1979) and Burland (1993) which were back calculated from field pile load test data. As shown, there is close agreement in the β values for the NC specimen for all three datasets. For an OCR of 4, the experimental and Burland (1993) β values are in close agreement, while for an OCR of 6, both the Esrig and Kirby (1979) and Burland (1993) values are greater than the experimental values. These differences could be due to soil disturbance effects during installation or to differences in drainage conditions.

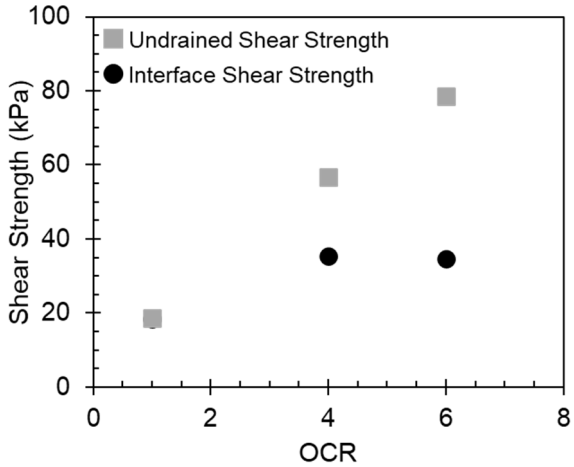

Figure 8. Interface shear strength and undrained shear strength as a function of OCR.

The ratio of τ_{int} to σ'_c is equivalent to the adhesion factor (α) used in design within the total stress framework, i.e. $\tau_{int}/\sigma'_c = \alpha$. The experimental results, shown in Fig. 9b, show a decrease in α with increasing OCR. The results are in close agreement with the relationship proposed by Randolph and Murphy (1985):

$$\alpha = \left(\frac{S_U}{\sigma'_c}\right)_{NC}^{0.25} \left(\frac{S_U}{\sigma'_c}\right)_{OC}^{-0.50} \quad (2)$$

For both the experimental and Randolph and Murphy (1985) values, the decrease in α with OCR reflects the increase in slippage at the interface.

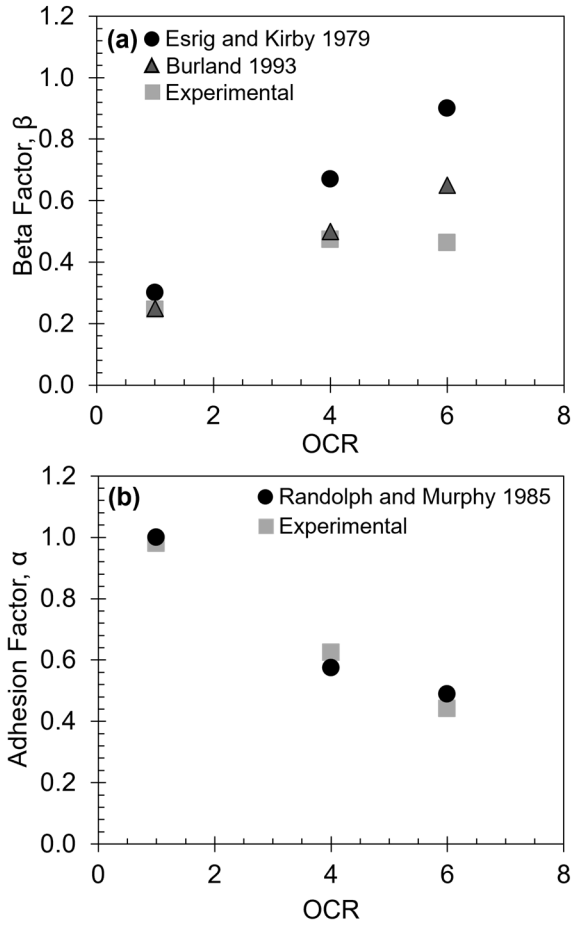

Figure 9. Deduced (a) adhesion factor and (b) β factor as a function of OCR and comparison with published values.

4. Conclusions

This paper describes a new interface shear setup equipped with a porous element at the soil-structure interface that enables measurements of excess pore pressures. The results of undrained tests on normally consolidated and overconsolidated specimens are presented, showing that the normally consolidated specimen generated positive excess pore pressures while the overconsolidated specimens generated negative excess pore pressures. These differences led to the mobilization of smaller interface shear strength by the normally consolidated specimen. Measurements of the excess pore pressures allow calculation of the vertical effective stresses, which were greater during the tests on the overconsolidated specimens. Calculated ratios of interface shear strength to current vertical effective stress show the greater peak values mobilized by the overconsolidated specimens due to their dilative tendencies accompanied by smaller residual values, likely due to the greater slippage taking place at the soil-structure interfaces of these specimens. At the residual state, the undrained and drained stress path of the normally consolidated specimens converges to the failure envelope. The results were used to deduce deep foundation design parameters used within the effective and total stress frameworks. The β values increased as the OCR increased in general agreement with published values. The α values decreased with OCR in close agreement with published values.

References

Boukpeti, N. and White, D. J. (2017). "Interface shear box tests for assessing axial pipe–soil resistance." Géotechnique, 67, no. 1: 18–30, https://doi.org/10.1680/jgeot.15.P.112.

Burland J.P. 1993 Closing address. In proceedings of recent large-scale fully instrumented pile tests in clay. Institute of Civil Engineers, London, 590–595

Esrig, M.I. and Kirby, R.C. 1979. "Soil capacity for supporting deep foundation members in clay." In Behavior of Deep Foundations, ASTM STP 670, edited by R. Lundgren, 27-63. 104. West Conshohocken, PA: ASTM International.

Jardine, R. J. and Lehane, B. M. 1992. "Residual strength characteristics of Bothkennar clay". Géotechnique, 42, no. 2: 363–367, https://doi.org/10.1680/geot.1992.42.2.363

Ladd, C. C. and Foott, R. 1974. "New design procedure for stability of soft clay." J. Geotech. Engng Div. 100, no. FT7: 763–786.

Lemos, L. J. L. and Vaughan, P. R. 2000. "Clay – interface shear resistance." Géotechnique 50, no. 1: 55–64, https://doi.org/10.1680/geot.2000.50.1.55.

Martinez, A. and Stutz, H.H. 2019. "Rate effects on the interface shear behaviour of normally and overconsolidated clay." Géotechnique, 69, no. 9: 801-815. https://doi.org/10.1680/jgeot.17.P.311

Randolph, M.F. and Murphy, B.S. 1985. "Shaft capacity of driven piles in clay." In Offshore Technology Conference, https://doi.org/10.4043/4883-MS

Stutz, H.H. and Martinez, A. 2018. "Meso- and macro-scale response of clay-structure interfaces under varying shearing rates. In IS-Atlanta Micro to Macro, 1-5.